The electromagnetically excited resonance of the pinion in fully-suspended drive of a locomotive and its sensitivity on the torsion stiffness of the rotor shaft

Vojtěch Dybala[1,*]

[1] *ČVUT v Praze, Fakulta strojní, Ústav automobilů, spalovacích motorů a kolejových vozidel, Technická 4, 166 07 Praha 6, Česká republika*

Abstract

The phenomenon of torsion oscillations in traction drives of modern high-power locomotives has been studied at the CTU in Prague. The ongoing research goes two ways with respect to the excitation of danger torsion oscillations – to study the influence of the adhesion phenomenon on these oscillations and to study the influence of harmonic components of the electromagnetic torque of an asynchronous traction motor. This contribution deals with the second approach. The harmonic components of the electromagnetic torque are presented as a ripple of the torque and has its origin in the ripple of asynchronous motor current. Within the article the focus will be put on both the study of sensitivity of the pinon resonance on the torsion stiffness of the rotor shaft as well as the approach how such study was realized. The conclusion of this contribution is on the summary of results of this study and defining of subsequent goals of this research.

Keywords: asynchronous motor; electromagnetic torque; torque ripple, harmonics, torsion oscillation, locomotive, fully-suspended

1. Introduction

A locomotive as any railway vehicle is a complex whole. Within the research and the subsequent creation of mathematical simulation models it was necessary to split it into fundamental parts – Electrical part, Mechanical part and Wheel-rail contact, see Fig. 1.

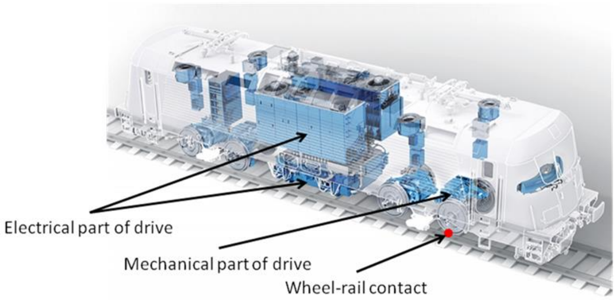

Fig. 1*- Fundamental structure of traction equipment [1]*

Based on this basic idea two mathematical models were built. The basic calculation model was created in MATLAB and the complex simulation model was created in MATLAB Simulink. While the basic calculation model is intended to provide basic characteristics of the mechanical torsion system as natural frequencies and natural modes of oscillations, the complex simulation model is intended to simulate the acceleration and the drive of the train and provide simulation data for subsequent analysis of excited oscillation states, e.g. magnitude analysis, frequency analysis of torques. The basic model works just with the free torsion system without implementing of the wheel-rail contact. On the other hand, the complex model includes this calculation submodel as well as the submodel, which deals with the dynamics of the train drive.

2. Description of mathematical models

2.1. Basic mathematical model

The basic mathematical model represents only the mechanical part of the locomotive drive. A typical example of such a fully-suspended drive can be seen on Fig. 2.

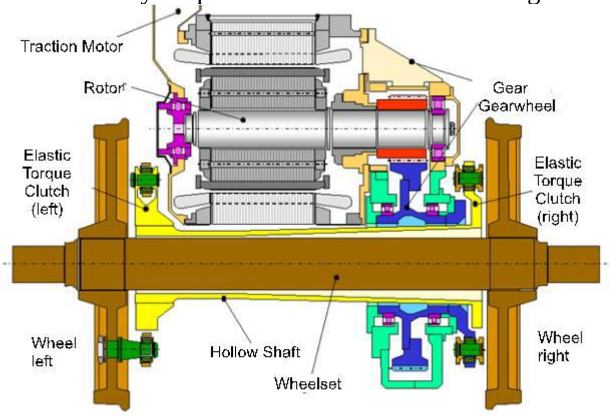

Fig. 2 Fully-suspended wheel-set drive - cross section [2]

In principle the fully-suspended drive was reduced on a torsion system (Fig. 3) for purposes of the basic calculation model creation.

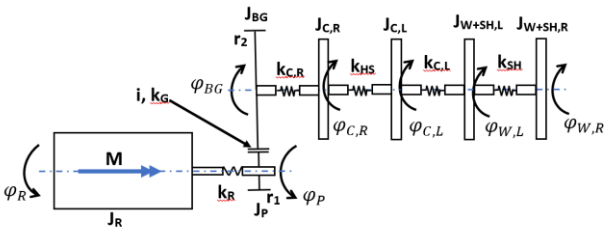

Fig. 3 Fully-suspended wheel-set drive - torsion system scheme

[*] Kontakt na autora: vojtech.dybala@fs.cvut.cz

For this scheme the Lagrange method to build equations of motion was applied. These equations of motion describe the system of the fully-suspended drive when the influence of the slipping forces acting in the wheel-rail contact is neglected. The matrix representation of them is (1). Above mentioned basic characteristics of the torsion system – natural frequencies and natural modes are received from a solution of equation system without the excitation [M] – system according to (2).

$$[J][\ddot{\varphi}] + [k][\varphi] = [M] \tag{1}$$

$$[J][\ddot{\varphi}] + [k][\varphi] = [0] \tag{2}$$

To solve the system (2) the MATLAB function *[eigenvector, eigenvalue] = eig.(k,J)* was applied. This function provides the vector of amplitudes of torsion oscillations when oscillation by *j* natural angle frequency Ωj = sqrt(λj) for its natural modes and the function provides eigenvalues λ as well. The eigenvalues must be recalculated on the natural frequencies *f* according to the formula (3).

$$f = \frac{\sqrt{\lambda}}{2\pi} \tag{3}$$

2.2. Complex mathematical model

This mathematical model was built in MATLAB Simulink and consists of four main submodels. Because of its extensiveness it is not feasible to present it here in its whole extend, but just with help of its layout (Fig. 3) and description of the main submodels. For more details about its creation and function [1] [2] [3] can be read.

2.2.1. Electrical part

The electrical part respects the control scheme layout as in Fig. 4. The structure controls parameters of the model of the asynchronous traction motor based on the required input – required torque *M**.

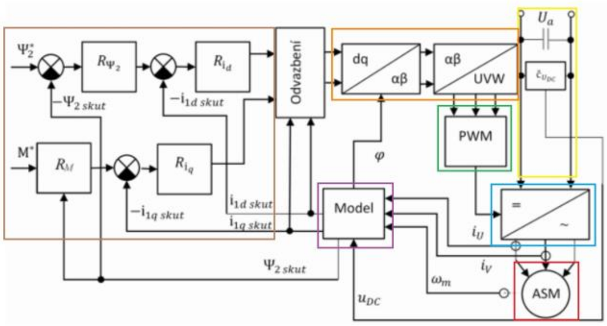

Fig. 4 Scheme of vector control [4]

2.2.2. Mechanical part

The arrangement of the mechanical part – the torsion system of the fully-suspended drive – is based on the scheme in Fig. 3. Modelling of this submodel is based on the idea of a block, which consists of a rotation mass, torsion stiffness and torsion damping element, see Fig. 6. From the mathematical point of view this kind of a block is described by the equation (4).

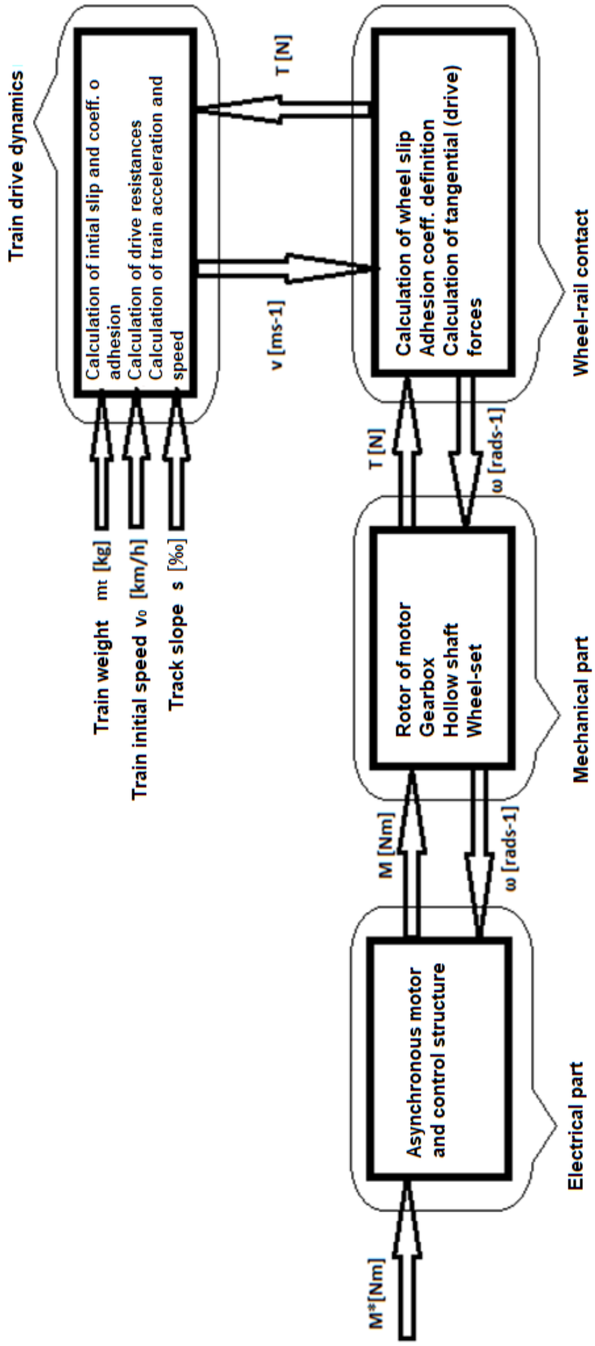

Fig. 5 Complex model layout

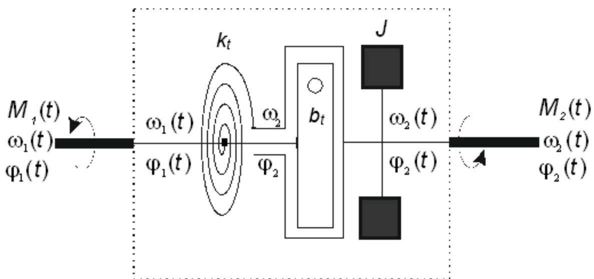

Fig. 6 Scheme for modelling of rotation mass, torsion stiffness and torsion damping [5]

$$J\dot{\omega}_2(t) = M_1(t) - M_2(t) = b_t(\dot{\varphi}_1(t) - \dot{\varphi}_2(t)) - k_t(\varphi_1(t) - \varphi_2(t)) - M_2(t) \tag{4}$$

2.2.3. Wheel-rail contact

The interaction in the wheel-rail contact is based on the principle of the phenomenon of adhesion. In this case the adhesion is represented by the Popovici's definition (Fig. 7). The coefficient μ is defined as a function of a wheel slip *s*. Popovici defines its own formula (5). The wheel slip *s* represents the difference between a real longitudinal speed of a vehicle and a speed, which correspond to an angle speed of wheels. For purposes of this simulation model only longitudinal slip s_x (6) is calculated. It means that the lateral slip s_y and a wheel spin due to sinus-movement of a wheel-set are neglected.

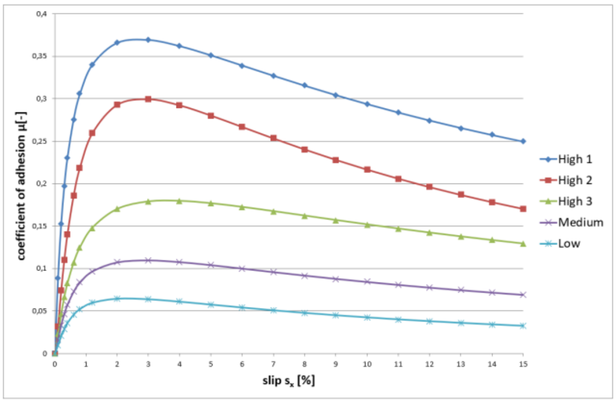

Fig. 7 Popovici's adhesion characteristics [6]

$$\mu = \mu_{MAX} e^{\frac{(ln(s_x)-b)^2}{c}} \tag{5}$$

$$s_x = \frac{r_k\omega_k - v_x}{v} \tag{6}$$

When the slip s_x and the coefficient of adhesion μ_x is known as well as the wheel force *Q*, the tangential force in the wheel-rail contact T_1 (Fig. 8), which accelerates the vehicle in the longitudinal direction, can be calculated according to the formula (7).

$$T_1 = Q\mu \tag{7}$$

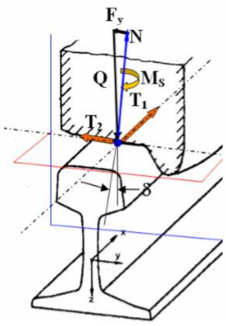

Fig. 8 Wheel-rail contact forces [7]

2.2.4. Train drive dynamics

This submodel solves group of analytical formulas.

The calculations lead to determination of the speed of the simulated train drive. The calculations are based on the balance between accelerating forces and resistance forces. In the first group of calculations the initial traction torque $M_{W,0}$ is calculated. This torque ensures the balance with initial vehicle resistances and is a part of the required value of torque *M**. The second group of calculations leads to the calculation of the train model speed (8), which consists of the defined initial speed and speed integrated from the acceleration of the modelled train.

$$v = v_0 + \int_0^t a\,dt \tag{8}$$

3. Simulations and results

3.1. Basic characteristics of the torsion system

For the supposed torsion system (Fig. 3) seven natural frequencies of torsion oscillations were calculated, see Table 1. The first one 0Hz represent own free rotation of the torsion system.

Table 1 Overview of natural frequencies

Natural frequencies of torsion system [Hz]						
1.	2.	3.	4.	5.	6.	7.
0	6	57	337	572	857	2403

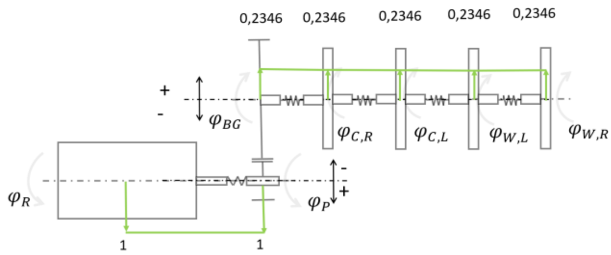

Fig. 9 First natural mode of torsion oscillations

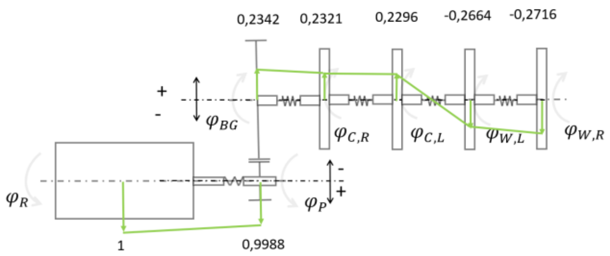

Fig. 10 Second natural mode of torsion oscillations

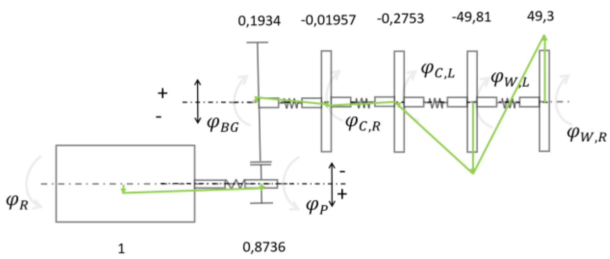

Fig. 11 Third natural mode of torsion oscillations

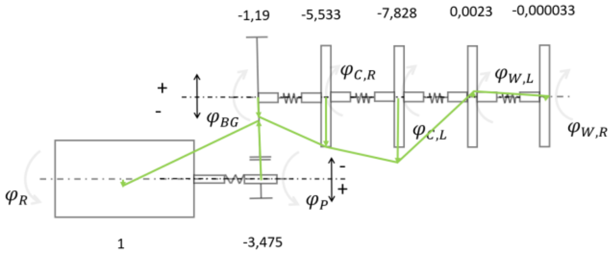

Fig. 12 Fourth natural mode of torsion oscillations

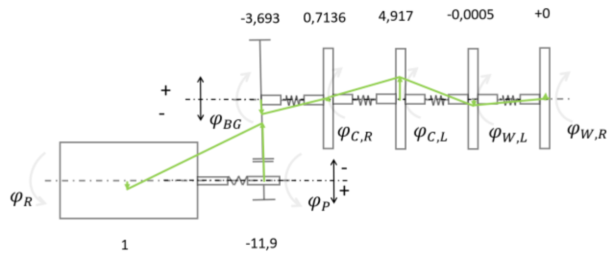

Fig. 13 Fifth natural mode of torsion oscillations

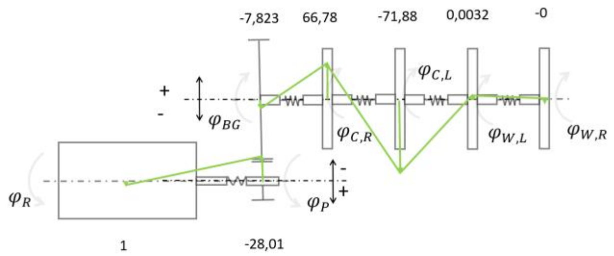

Fig. 14 Sixth natural mode of torsion oscillation

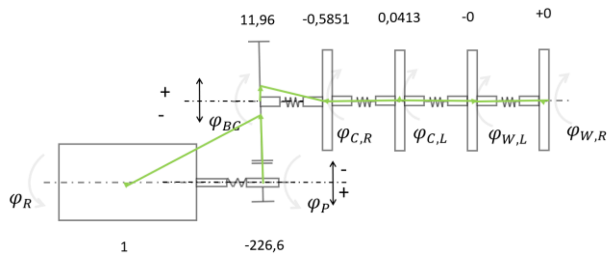

Fig. 15 Seventh natural mode of torsion oscillations

For those seven natural frequencies of torsion oscillations there are corresponding natural modes of torsion oscillations - Fig. 9 to Fig. 15. For purposes of subsequent research, a description of natural modes of torsion oscillations was put together - Table 2.

Table 2 Description of natural modes

Order of natural modes	Respective natural frequency [Hz]	Dominant oscillations of a mass	Less significant oscillations
1.	0	Own free rotation	-
2.	6	Wheel-set towards hollow shaft	-
3.	57	Wheels of wheel-set	-
4.	337	Wheel-set towards hollow shaft	Pinion towards rotor
5.	572	Pinion towards rotor	-
6.	857	Hollow shaft joints	Wheel-set towards hollow shaft Gear wheel towards hollow shaft
7.	2403	Pinion towards rotor Pinion towards gear wheel	-

3.2. Analysis of electromagnetic torque and resonance excitation

The main goal of the first simulation with the complex model was to gain information about the representation of harmonic components in the electromagnetic torque of the model of the asynchronous motor. Fig. 16 represents the course of the electromagnetic torque, which acts on the rotor during this kind of a basic simulation. Within this simulation the train accelerated up to maximal torque to reach speed app. 50 km/h and then the torque was reduced to keep the train on this speed. For the steady state the FFT analysis (Fast Fourier Transformation) of the electromagnetic torque was performed.

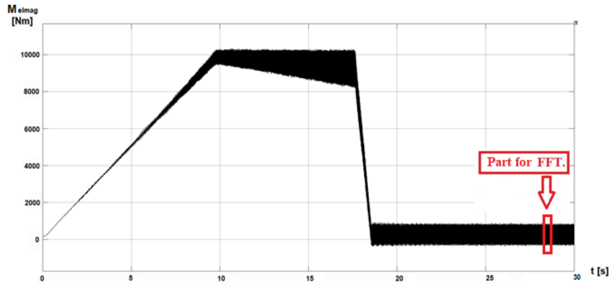

Fig. 16 Course of electromagnetic torque of model of asynchronous motor

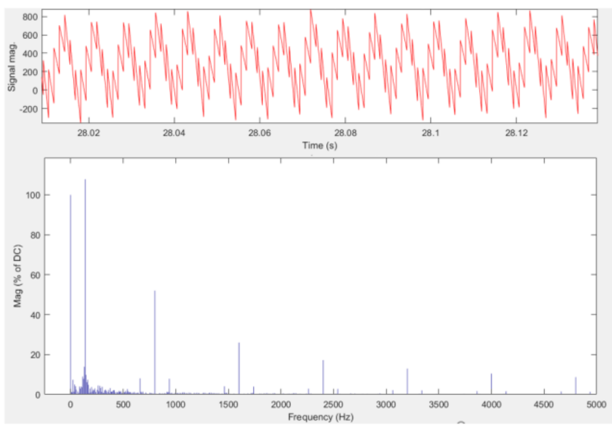

Fig. 17 Graphical presentation of FFT analysis

FFT analysis (Fig. 17) revealed the presence of many harmonic components. These harmonic components have its origin in switching of semiconductors in the model of an inverter and causing a ripple of motor currents and subsequently a ripple of the electromagnetic torque.

Table 3 Overview and description of apparent frequencies of electromagnetic torque

Apparent frequency [Hz]	Magnitude of apparent frequency towards magnitude of DC/nominal component of signal [%]	Phenomenon description
138	104	3th multiple of f_1 (1st harmonic of supply voltage)
800 and its multiples	55 až 10	Even and odd multiples of switching frequency f_{PWM}
+/-138	8 až 0	Sidebands of all multiples of switching frequency

The knowledge of natural frequencies and frequencies of harmonic components of the electromagnetic torque, which are supposed to excite torsion oscillations, enables to create the Campbell diagram (Fig. 18). This diagram reveals five potential areas, where resonance of torsion oscillations can occur. These are areas where a natural frequency meets a frequency of a harmonic component of the electromagnetic torque. Based on this knowledge other simulations were carried out. These simulations were focused on the excitation of supposed resonances. Therefore, the train was accelerated within the speed range, where the potential resonances are identified by the Campbell diagram. The acceleration was realized by maximal electromagnetic torque, see Fig. 19.

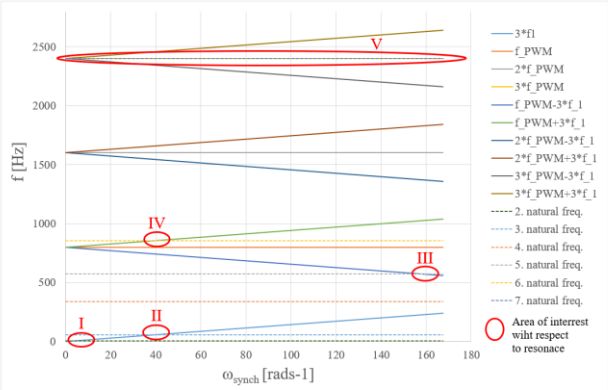

Fig. 18 Campbell diagram

The Fig. 19 shows that the ripple of the torque increase with speed. This effect is given by the fact that the modulation of the supply voltage is getting worse as a function of rotation speed. Fig. 20 presents that there was excited enormous resonance state. The FFT analysis (Fig. 21) revealed a frequency component with the frequency of 573Hz and magnitude of almost 90% of the nominal value of the torque. The resonance was detected in 26,9 seconds. At that time the rotation speed of the rotor was 154 rad. s^{-1} or 24,5 Hz.

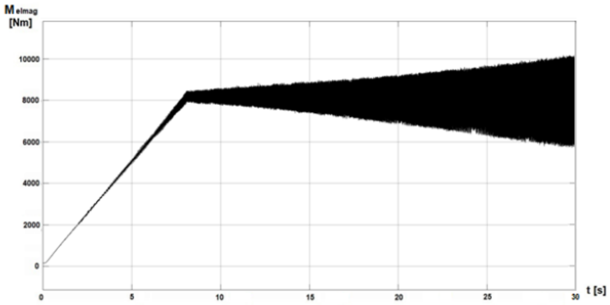

Fig. 19 Course of electromagnetic torque of model of asynchronous motor

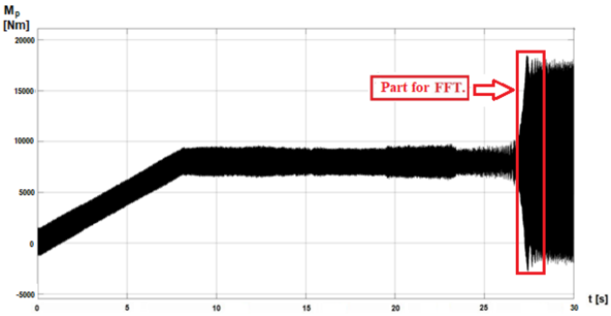

Fig. 20 Course of pinion acceleration torque

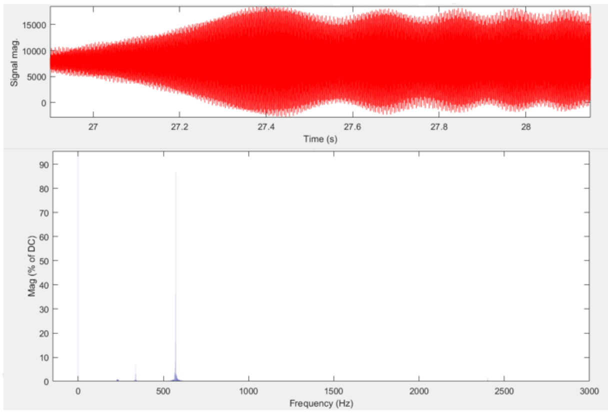

Fig. 21 Graphical presentation of FFT analysis

The respective frequency of the first harmonic of the supply voltage f_1 was 76Hz. If the third multiple of f_1 = 228Hz is subtracted from the first multiple of switching frequency f_{PWM} = 800Hz the result is 572Hz. According to Table 3 it can be deduced that 572Hz corresponds to a frequency sideband and it is the resonance state III according to the Campbell diagram. So, there is a clear concurrence. On the other hand, there is also a potential of the resonance state named V in the Campbell diagram. This one is not clear resonance in fact, as the natural frequency is 2403Hz and the third multiple of switching frequency is 2400Hz. But they are very close within the whole speed range, so it was supposed this one should arise. It did not happen. Because the resonances named I, II and IV are not linked to the oscillations of pinion there will be put no interest on them in the following text. To explain the lack of clarity from resonance state V other simulations were needed. Next step was to get the information how magnitudes of the relevant harmonic components are dependent on the rotation speed. Results of these simulations (Fig.

22) shows strong dependence. Based on this it was supposed, that harmonics of low frequencies have no sufficient magnitude or potential to excite a resonance, but the resonance V should appear according to these results.

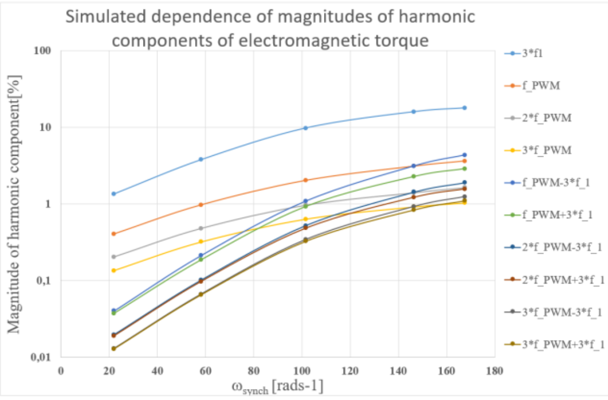

Fig. 22 Magnitude of harmonic component as a function of rotation speed

To see if there is a dependence of magnitude of excited oscillations with frequencies of fifth and seventh natural frequency a sensitivity analysis was carried out. This sensitivity test is based on tuning of values of fifth and seventh natural frequency due to change of the torsion stiffness of the rotor shaft, which connects the rotation mass of the rotor with the rotation mass of the pinion. This torsion stiffness is named k_R in the Fig. 3. The sequence of values of these stiffnesses is presented in Table 4 below as well as respective values of natural frequencies. The basic value, used in previous simulations, is marked k_{R0}. The others are defined as ratio in (%).

Table 4 Applied set of rotor torsion stiffnesses

Order marking	Ration between particular torsion stiffness and the basic one – k_{RX}/k_{R0} [%]	Natural frequency [Hz]	
		5.	7.
k_{R1}	80	540	2355
k_{R2}	90	556	2378
k_{R0}	100	572	2403
k_{R3}	110	589	2428
k_{R4}	120	603	2452
k_{R5}	130	617	2477
k_{R6}	140	630	2501
k_{R7}	150	642	2525
k_{R8}	160	653	2548
k_{R9}	170	665	2573
k_{R10}	180	675	2597
k_{R11}	190	685	2621
k_{R12}	200	694	2646
k_{R13}	210	702	2668

In Fig. 23 it can be seen, that the natural frequencies have a linear dependence on the tuning of the torsion stiffness of the rotor. Results of this batch of simulations are presented in Fig. 24 and Fig. 25.

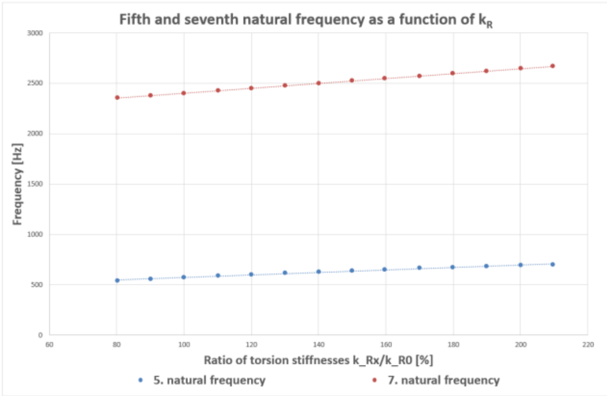

Fig. 23 Natural frequencies as a function of rotor torsion stiffness

Specifically, the Fig. 24 revealed that there is clear linear dependency of the magnitude of harmonic component in the resonance state of the fifth natural frequency. The magnitude varies from app. 90% for lower stiffness (lower natural frequency) to app. 10% for higher stiffness (higher frequency). This corresponds the Campbell diagram (Fig. 18) as well as with the Fig. 22. It means shifting of the fifth natural frequency to higher values shifts the resonance state III to lower speed where is lower potential of harmonic component of the electromagnetic torque to excite a strong resonance and vice versa.

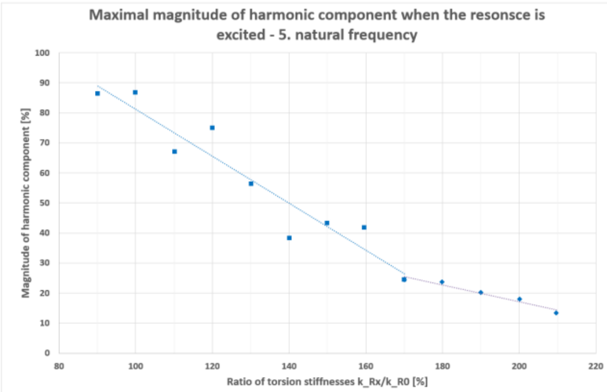

Fig. 24 Magnitude of resonance oscillation as a function of k_R

In case of the seventh natural frequency the study of the magnitude as a function of the torsion stiffness k_R (Fig. 25) shows that the resonance was not excited in no case. The figure presents kind of a linear dependence, but the magnitude varies within a range of few percent. In comparison with the situation for the resonance state of the fifth natural frequency this can be considered as constant dependency and it is clear there is no resonance for the seventh natural frequency, just kind of a forced torsion oscillations.

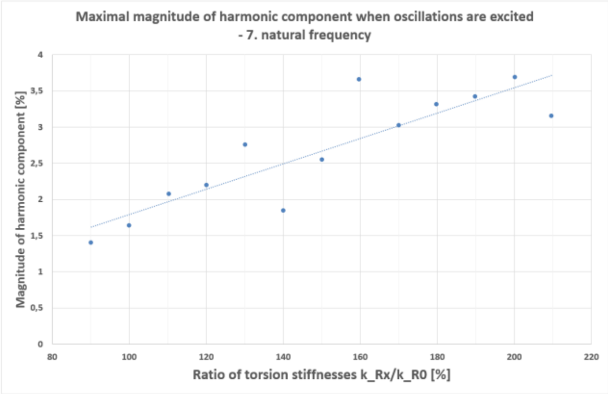

Fig. 25 Magnitude of oscillation as a function of k_R

4. Conclusion

The presented simulations in the complex simulation model shows that there is a big potential of excitation of danger resonance states for the torque, which loads the pinon of the gearbox in the fully-suspended drive of a locomotive. Magnitudes of these resonance oscillations can reach high tens of percent. There is also still an open question regarding the excitation of the torsion oscillations of the pinion loading torque for high natural frequencies. It seems according to the Fig. 22, that the frequency sideband of the third multiple of the switching frequency f_{PWM} has an equivalent potential to excite a resonance oscillations V on the seventh natural frequency in higher rotation speeds as it is for the resonance state III. This investigation will be the next step to try to find a sensitivity of the resonance excitation on the natural frequency of the torsion system. Regarding the basic calculation model that will be also updated with respect to the influence of the wheel-rail contact. In these days the torsion system in this calculation model is supposed to be a "free" system without this interaction. But the connection between wheels and rails shall be implemented via elements of springs and dampers. As the damping in the contact is a function of a velocity there shall be studied its impact on frequency retuning of the torsion system.

Acknowledgement

This research has been realized using the support of The Technology Agency of the Czech Republic, programme National Competence Centres, project # TN01000026 Josef Bozek National Center of Competence for Surface Transport Vehicles and the support of The Czech Technical University and the related grant – No. SGS20/120/OHK2/2T/12.
This support is gratefully acknowledged.

List of symbols

a	acceleration ($m.s^{-2}$)
b	Popovici's fit parameter (-)
b_t	torsion damping ($Nms.rad^{-1}$)
c	Popovici's fit parameter (-)
f	frequency (Hz)
f_{PWM}	PWM frequency (Hz)
f_1	1st harmonic frequency (Hz)
J	mass of inertia (kgm^{-2})
$[J]$	matrix of masses of inertia (kgm^{-2})
k_R	torsion stiffness of a rotor ($Nm.rad^{-1}$)
k_t	torsion stiffness generally ($Nm.rad^{-1}$)
$[k]$	matrix of torsion stiffnesses ($Nm.rad^{-1}$)
M_1	input torque (Nm)
M_2	output torque (Nm)
$[M]$	matrix of external torques (Nm)
$M_{W,0}$	initial wheel-set torque (Nm)
Q	vertical wheel force (N)
r_k	wheel radius (mm)
s	wheel slip (-)
s_x	wheel slip in longitudinal direction (-)
s_y	wheel slip in lateral direction (-)
t	time (s)
T_1	tangential longitudinal force (N)
v	velocity ($m.s^{-1}$)
v_0	initial velocity ($m.s^{-1}$)
λ	eigenvalue (-)
Ω	natural angle frequency ($rad.s^{-1}$)
ω_k	wheel angular speed ($rad.s^{-1}$)
$\dot{\omega}$	time derivative of angular speed ($rad.s^{-2}$)
φ_1	input angle rotation (rad)
φ_2	output angle rotation (rad)
$[\varphi]$	matrix of angle rotations (rad)
$\dot{\varphi}_1$	time derivative of input angle rotation (rad.s-1)
$\dot{\varphi}_2$	time derivative of output angle rotation (rad.s-1)
$[\ddot{\varphi}]$	matrix of second time derivative of angle rotations (rad)
μ	coefficient of adhesion (-)
μ_{MAX}	max. value of coefficient of adhesion (-)
μ_X	adhesion coefficient in longitudinal direction (-)

Disclosure statement

The content of this paper does not infringe any copyrights, patents, know-how of anybody else or rules of the grant provider.

The tutor of the author is doc. Ing. Josef Kolář, CSc., U 12 120, FS ČVUT v Praze: josef.kolar@fs.cvut.cz

Reference

[1] V. Dybala, „Vliv regulace na frekvenční složení fázových proudů a elektromagnetického momentu při simulování napájení asynchronního motoru ze střídače," v Súčasné problémy v koľajových vozidlách - PRORAIL 2019. Diel I, Žilina, 2019.

[2] V. Dybala, M. Libenský, B. Šulc a C. Oswald, „Slip and Adhesion in a Railway Wheelset Simulink Model Proposed for Detection Driving Conditions Via Neural Networks," v SBORNÍK vědeckých prací Vysoké školy báňské - Technické univerzity Ostrava, Řada strojní, Ostrava, 2018.

[3] V. Dybala, „Simulace zvlnění elektromagnetického momentu asynchronního trakčního motoru lokomotivy napájeného ze střídače," v Sborník konference STČ na Strojní fakultě ČVUT v Praze, Praha, 2019.

[4] T. Fridrichovský, „Studie disertační práce," Praha, 2017.

[5] T. Fridrichovský a B. Šulc, „Investigation of Torsional Oscillations in Railway Vehicles," 21 October 2016. [Online]. Available: Dostupné z: https://doi.org/10.1051/matecconf/20167602052. [Přístup získán 2018].

[6] R. I. Popovici, Friction in Wheel - Rail Contacts, Enschede, The Netherlands : University of Twente, 2010.

[7] J. Kalivoda, „Teorie vozidel," Fakulta strojní ČVUT v Praze, Praha, 2019.

[8] J. Javůrek, Regulace moderních elektrických pohonů, Praha: Grada Publishing, a.s., 2003.